PTEP

Prog. Theor. Exp. Phys. **2023** 043B01(27 pages)
DOI: 10.1093/ptep/ptad042

IYBSSD2022
International Year
of Basic Sciences
for Sustainable Development

On the existence of the NS5-brane limit of the plane wave matrix model

Yuhma Asano [1,2,*], Goro Ishiki[1,2], Takaki Matsumoto [3], Shinji Shimasaki, and Hiromasa Watanabe [4]

[1] *Graduate School of Pure and Applied Sciences, University of Tsukuba, Tsukuba, Ibaraki 305-8571, Japan*
[2] *Tomonaga Center for the History of the Universe, University of Tsukuba, Tsukuba, Ibaraki 305-8571, Japan*
[3] *School of Theoretical Physics, Dublin Institute for Advanced Studies, 10 Burlington Road, Dublin 4, Ireland*
[4] *Yukawa Institute for Theoretical Physics, Kyoto University, Kyoto 606-8502, Japan*
*E-mail: asano@het.ph.tsukuba.ac.jp

Received December 7, 2022; Revised March 8, 2023; Accepted March 14, 2023; Published March 24, 2023

We consider a double scaling limit of the plane wave matrix model (PWMM), in which the gravity dual geometry of PWMM reduces to a class of spherical NS5-brane solutions. We identify the form of the scaling limit for the dual geometry of PWMM around a general vacuum and then translate the limit into field-theoretic language. We also show that the limit indeed exists at least in a certain planar quarter-BPS sector of PWMM by using the localization computation analytically. In addition, we employ the hybrid Monte Carlo method to compute the matrix integral obtained by the localization method, near the parameter region where the supergravity approximation is valid. Our numerical results, which are considered to be the first computation of a quantum loop correction to the Lin–Maldacena geometry, suggest that the double scaling limit exists beyond the planar sector.

Subject Index B21, B25

1. Introduction

The gauge/gravity correspondence claims equivalence between a certain class of gauge theories and string theories [1–3]. The dual description provided by this relation often gives a useful method of analyzing the gauge theories and string theories. This is also applicable to the little string theory (LST), which is considered to be defined on NS5-branes in the decoupling limit (see Refs. [4,5] and references therein). Although any direct definition of LST using a Lagrangian has not been established yet, the gravity description enables us to extract information on LST.

Based on the gauge/gravity duality, it was conjectured that the type IIA LST on $R \times S^5$ is described by the plane wave matrix model (PWMM) [6] in a double scaling limit [7,8], which we call the "NS5-brane limit" in this paper. The gravity dual of PWMM possesses a scaling limit where the geometry reduces to an NS5-brane solution. If the gauge/gravity correspondence is

Funded by SCOAP[3]. SCOAP3 and OUP support the goals of the International Year of Basic Sciences for Sustainable Development

true, it implies that the limit also exists on the (gauge-)field theory side. Thus, the IIA LST is expected to be described as this limit of PWMM. Since PWMM is a well-defined matrix quantum mechanics, this relation is expected to give a direct definition of the LST. In this paper, we investigate this relation.

The gauge/gravity duality in this context is for theories with $SU(2|4)$ symmetry. The field theory side in this duality consists of PWMM, $\mathcal{N} = 8$ SYM on $R \times S^2$, $\mathcal{N} = 4$ SYM on $R \times S^3/Z_k$, and the IIA LST on $R \times S^5$ [7] (see also Refs. [9–11]). These theories have many discrete vacua, which preserve the $SU(2|4)$ symmetry. The vacua in PWMM are given by fuzzy spheres and classified by the representation of the $SU(2)$ Lie algebra. For SYM on $R \times S^2$ and SYM on $R \times S^3/Z_k$, the vacua are labeled by monopole charges and holonomy, respectively. The description of the vacua of the IIA LST is not clear due to the lack of a direct definition of the theory. However, from the gravity description, one can find that each non-trivial vacuum of the LST carries not only the NS5-brane charges but also some D2-brane charges[1].

For each vacuum of these theories, the $SU(2|4)$ symmetric dual geometry was constructed [7]. This class of geometries has $R \times SO(3) \times SO(6)$ isometry, and they locally contain $R \times S^2 \times S^5$. A remarkable feature is that the equations that determine those geometries can be rewritten into the form of Laplace equations in certain axially symmetric electrostatic systems. The system consists of background potential and a set of conducting disks, which specify the corresponding field theory and a vacuum of the theory, respectively. The geometry is completely fixed by the electrostatic potential of the system.

The geometry dual to the IIA LST is a gravity solution for spherical NS5-branes. It was pointed out that this NS5-brane geometry can be obtained by taking a limit of the dual geometry of PWMM such that one of the conducting disks becomes infinitely large [7,8]. Then, this limit is translated into the language on the field theory side, and found to be a certain double scaling limit in PWMM, in which the 't Hooft coupling also becomes large as the matrix size approaches infinity. Through the gauge/gravity correspondence, this relation suggests that the IIA LST is realized as the double scaling limit of PWMM. The same argument can also be made for $\mathcal{N} = 8$ SYM on $R \times S^2$ and $\mathcal{N} = 4$ SYM on $R \times S^3/Z_k$ [13].

The form of the double scaling limit was only found for the case of a simple vacuum of PWMM [8]. In this case, the resulting IIA LST is the theory around the trivial vacuum of the LST, which has only one stack of 5-branes. In this paper, we generalize this argument to the situations where the IIA LST around a general non-trivial vacuum are realized, which also carries some D2-brane charges. We find the form of the double scaling limit in general gravity solutions and then rewrite it using field-theoretic parameters.

For this purpose, we use the remarkable result found in Refs. [14,15] based on the localization computation[2], which states that the eigenvalue distribution of an adjoint scalar field on the gauge theory side is identified with the charge densities on the conducting disks. Through this relation, we can identify the parameters on both sides and express the double scaling limit in terms of the parameters of PWMM. Furthermore, the direct identification between the eigenvalue densities and the charge densities also makes it possible to see that the double scaling limit exists at least in the planar quarter-BPS sector of PWMM that is considered in the localization computation.

[1] These branes are compact, so that the net brane charge must be vanishing in the matrix theory description [12]. By the "brane charges", we mean the local dipole charges in this paper.

[2] Beside this result [14,15], there are some applications of the localization computation [16–18].

In addition to the analytic computation, we numerically compute the quantities of the BPS sector in PWMM with finite matrix size N by applying the hybrid Monte Carlo method to the matrix integral obtained in the localization computation. Such numerical computation allows us to discuss the double scaling limit beyond the planar sector because it can provide information on $1/N$ corrections. As a result of the numerical computation, we find evidence that the double scaling limit seems to exist at the non-planar level.

This paper is organized as follows. In Sect. 2, we review how the dual geometry is related to the electrostatic system. In Sect. 3, we consider the double scaling limit, in which the dual geometry of PWMM is reduced to an NS5-brane solution. We first review the simplest case obtained in Ref. [8] and then generalize it to the cases for non-trivial vacua. In Sect. 4, after we review the correspondence between the scalar eigenvalue densities and the charge densities, we see how the double scaling limit is realized on the gauge theory side. In Sect. 5, we present numerical results that support the existence of the double scaling limit. Finally, we summarize the paper in Sect. 6 with a discussion.

2. Dual geometries of PWMM and LST

The supergravity solutions dual to the (gauge) theories with $SU(2|4)$ symmetry were obtained in Refs. [7,9] by using an $SU(2|4)$ symmetric ansatz. The geometry is written by a single function $V(r, z)$, as

$$\begin{aligned}
ds_{10}^2 &= \left(\frac{\ddot{V}-2\dot{V}}{-V''}\right)^{1/2}\left\{-4\frac{\ddot{V}}{\ddot{V}-2\dot{V}}dt^2-2\frac{V''}{\dot{V}}(dr^2+dz^2)+4d\Omega_5^2+2\frac{V''\dot{V}}{\Delta}d\Omega_2^2\right\},\\
C_1 &= -\frac{(\dot{V}^2)'}{\ddot{V}-2\dot{V}}dt, \quad C_3 = -4\frac{\dot{V}^2V''}{\Delta}dt\wedge d\Omega_2,\\
B_2 &= \left(\frac{(\dot{V}^2)'}{\Delta}+2z\right)d\Omega_2, \quad e^{4\Phi} = \frac{4(\ddot{V}-2\dot{V})^3}{-V''\dot{V}^2\Delta^2},
\end{aligned} \tag{1}$$

where $\Delta = (\ddot{V}-2\dot{V})V''-(\dot{V}')^2$ and the dots and primes indicate $\frac{\partial}{\partial \log r}$ and $\frac{\partial}{\partial z}$, respectively. Note that the geometry contains $S^2\times S^5$, which reflects the bosonic subgroup $SO(3)\times SO(6)$ of $SU(2|4)$.

The supersymmetry requires $V(r, z)$ to satisfy

$$\frac{1}{r^2}\ddot{V}+V''=0. \tag{2}$$

The positivity and regularity of the metric impose further conditions. The positivity restricts the asymptotic behavior of $V(r, z)$ for large r and z. The regularity at the points where S^2 or S^5 shrinks to zero requires either one of the following conditions to be satisfied: (A) $\frac{\partial}{\partial r}V(r, z)\sim r$ at $r=0$ or (B) $z=$ constant if $\frac{\partial}{\partial r}V=0$. One can then construct a 3-cycle or 6-cycle that is a fiber bundle over a non-contractible curve connecting two points where S^2 or S^5 shrinks, with the fiber given by the sphere. The integrals of fluxes H_3 and $\star\tilde{F}_4$ over these cycles yield NS5-brane charges and D2-brane charges, respectively [7].

Equation (2), which determines $V(r, z)$, is just the Laplace equation in the axisymmetric 3D space and the regularity condition on $V(r, z)$ can be rephrased as the presence of some conducting disks. Thus, the geometry is described in terms of the axisymmetric electrostatic system with the conducting disks, and $V(r, z)$ is interpreted as an electrostatic potential. The positivity of the metric requires the existence of a background potential in the electrostatic system, which we will introduce explicitly in the following subsections.

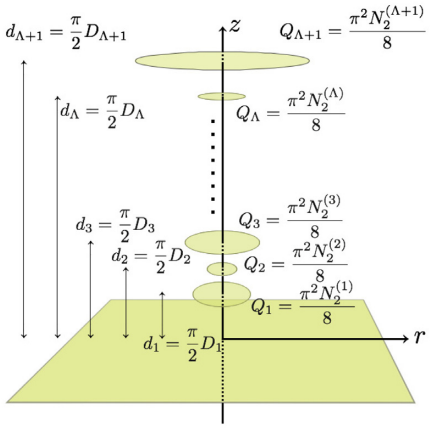

Fig. 1. The electrostatic system for a dual geometry of PWMM.

The electric charges and the z-coordinates of the conducting disks are parameters of this geometry. As we will describe in the next subsection, they are proportional to D2-brane and NS5-brane charges, respectively, through the cycle integrals, and are thus quantized. On the other hand, the radii of the disks are not free parameters of the solution, since the regularity of the solution requires that the charge density on any finite disk must vanish at the edge. This relates the radius of the disk to the charge.

2.1. *Dual geometry of PWMM*

In the following, we focus on the dual geometry of PWMM. In order for the solution to become the D0-brane geometry in the UV region, the presence of an infinite conducting plate (say at $z = 0$) is required[3]. Then only the space with $z > 0$ becomes relevant for this geometry. We also need a background potential of the form

$$V_{\rm bg}(r, z) = V_0 \left(r^2 z - \frac{2}{3} z^3 \right), \tag{3}$$

where V_0 is a positive constant. This is determined from the positivity of the metric. There are also some finite conducting disks along the z-direction. We denote the z-coordinate and the total electric charge of the sth disk by d_s and Q_s, respectively (Fig. 1). Through the cycle integrals mentioned above, these quantities are related to the NS5-brane charge of the sth stack $N_5^{(s)}$ and the D2-brane charge of the sth stack $N_2^{(s)}$ as

$$d_s = \frac{\pi D_s}{2}, \quad Q_s = \frac{\pi^2 N_2^{(s)}}{8}, \tag{4}$$

where $D_s = \sum_{t=1}^{s} N_5^{(t)}$.

The solution to the Laplace equation (2) generally takes the form [15,19]

$$V(r, z) = V_{\rm bg}(r, z) + \sum_{s=1}^{\Lambda+1} V_s(r, z), \tag{5}$$

where

$$V_s(r, z) = \frac{1}{\pi} \int_{-R_s}^{R_s} du \left(\frac{1}{\sqrt{(z - d_s + iu)^2 + r^2}} - \frac{1}{\sqrt{(z + d_s + iu)^2 + r^2}} \right) f_s(u). \tag{6}$$

[3]When the solution is lifted up to 11 dimensions, the infinite conducting plate is required in order for the asymptotic geometry to be the plane wave geometry.

f_s and R_s are the electric charge density and radius of the sth disk, respectively. The support of the function f_s is the interval $[-R_s, R_s]$. Let $\sigma_s(r)$ be the charge density along the radial direction on the sth disk. Then, it is related to f_s by

$$f_s(u) = 2\pi \int_{|u|}^{\infty} dr \frac{r\sigma_s(r)}{\sqrt{r^2-u^2}}, \qquad \sigma_s(r) = -\frac{1}{\pi^2} \int_r^{R_s} du \frac{f_s'(u)}{\sqrt{u^2-r^2}}. \tag{7}$$

These relations imply that f_s can be interpreted as the charge density projected onto a diameter of the disk. The regularity of the gravity solution requires that each charge density $\sigma_s(r)$ vanish at the tip of the disk or equivalently $\frac{d}{du} f_s(u)$ be finite at the edges.

In terms of these expressions, one can show that V_s satisfies the following differential equation:

$$\triangle V_s(r, z) = -4\pi\sigma_s(r)(\delta(z-d_s) - \delta(z+d_s)). \tag{8}$$

The total charge of the sth disk can be written as

$$Q_s = 2\pi \int_0^{R_s} r dr\, \sigma_s(r) = \frac{1}{\pi} \int_{-R_s}^{R_s} du\, f_s(u). \tag{9}$$

The Laplace equation (2) is rewritten in terms of the density $f_s(u)$ into the following integral equation:

$$f_s(u) - \sum_{t=1}^{\Lambda+1} (K_t(d_s+d_t) - K_t(|d_s-d_t|)) f_t(u) = C_s + \frac{2}{3} V_0 d_s^3 - 2V_0 d_s u^2, \tag{10}$$

where C_s is the constant value of the potential on the sth disk and K_s is defined by

$$K_s(\delta) f(u) := \frac{1}{\pi} \int_{-R_s}^{R_s} du' \frac{\delta}{\delta^2 + (u-u')^2} f(u'), \tag{11}$$

where δ is an arbitrary real number. See Refs. [14, 15, 19] for a derivation of Eq. (10). For general disk configurations, no analytic solution of Eq. (10) is known. However, in some scaling limits considered in Ref. [8], one can evaluate the charge density.

2.2. *Dual geometry of LST*

The electrostatic system for a general vacuum of LST consists of two infinite conducting plates at $z = 0$ and $z = d$ and some finite conducting disks placed between them. The positivity of the metric requires the presence of the background potential,

$$\tilde{V}_{\rm bg}(r, z) = \frac{1}{g_0} \sin\frac{\pi z}{d} I_0\left(\frac{\pi r}{d}\right), \tag{12}$$

where I_0 is the modified Bessel function of the 0th order, g_0 is a constant, and $0 \le z \le d$. The positions and charges of the disks are related to the brane charges in the same way as Eq. (4) (see Fig. 2).

The potential for this system can be written as

$$\tilde{V}(r, z) = \tilde{V}_{\rm bg}(r, z) + \sum_{n=-\infty}^{\infty} \sum_{s=1}^{\Lambda} \tilde{V}_{s,n}, \tag{13}$$

where Λ is the number of the finite conducting disks and

$$\tilde{V}_{s,n} = \frac{1}{\pi} \int_{-R_s}^{R_s} du \left(\frac{1}{\sqrt{(z-d_s+2nd+iu)^2+r^2}} - \frac{1}{\sqrt{(z+d_s+2nd+iu)^2+r^2}} \right) \tilde{f}_s(u). \tag{14}$$

$\tilde{f}_s$ represents the charge densities on the finite conducting disks. The infinite summation in the second term in Eq. (13) corresponds to contributions from infinitely many mirror images of

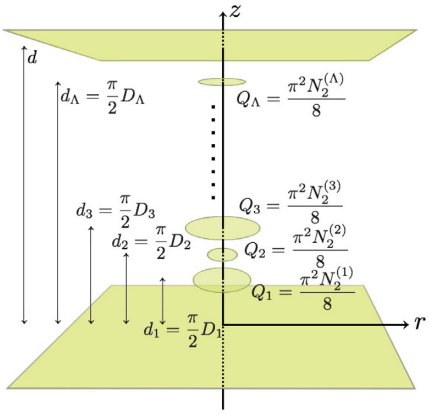

Fig. 2. The electrostatic system for a dual geometry of LST.

the conducting disks. The charge densities $\tilde{f}_s$ satisfy

$$\tilde{f}_s(u) - \sum_{n=-\infty}^{\infty} \sum_{t=1}^{\Lambda} (K_t(|d_s + d_t + 2nd|) - K_t(|d_s - d_t + 2nd|)) \tilde{f}_t(u) = \tilde{C}_s - \frac{1}{g_0} \sin \frac{\pi d_s}{d} \cosh \frac{\pi u}{d}, \tag{15}$$

where $\tilde{C}_s$ is the value of the potential on the sth disk and $K_s(d)$ represents the integral operator defined in Eq. (11).

If we consider the simplest case where there is no conducting disk between the two infinite plates, the geometry at large r reduces to the geometry with linear dilaton and H flux, which is a typical feature of NS5-brane solutions [8]. This fact enables us to associate this class of solutions with the NS5-branes. Note that for a generic disk configuration, the geometry possesses not only NS5-brane charges but also D2-brane charges.

3. NS5-brane limit on the gravity side

In this section, we consider the NS5-brane limit, in which the dual geometry of PWMM reviewed in Sect. 2.1 is reduced to the NS5-brane geometry in Sect. 2.2 as a result of a double scaling limit.

As reviewed in the previous section, the dual geometries of both PWMM and LST can be described in terms of electrostatic potentials of axisymmetric electrostatic systems (Figs. 1 and 2). Comparing two systems, one can find that the NS5-brane limit corresponds to the limit where the radius of the disk at the highest position in z in the electrostatic system for PWMM is sent to infinity. It turns out, however, that only taking this limit does not lead to the electrostatic system for LST. Indeed, in order to obtain the background potential of LST (12), one also needs to tune the magnitude of the background potential in a suitable manner. Thus, the NS5-brane limit turns out to be a double scaling limit.

The NS5-brane limit for the trivial vacuum of LST (i.e., the case without any finite conducting disks) was first investigated in Ref. [8]. Here, we extend this study to the case for a general vacuum.

3.1. *NS5-brane limit for the trivial vacuum*

Let us first review the NS5-brane limit for the trivial vacuum of LST [8]. The electrostatic system in this case consists of two infinite conducting plates and the background potential (12) (Fig. 2 with $\Lambda = 0$). Since there are no charged disks, the potential of this system is given only by the background potential (i.e., the first term in Eq. (13)). We will show that this electrostatic system can be obtained as a double scaling limit of the particular electrostatic system for PWMM, which consists of a single finite conducting disk and the infinite plate (Fig. 1 with $\Lambda = 0$).

In the electrostatic system of PWMM, let Q, R, and d be the total charge, the radius, and the z-coordinate of the conducting disk, respectively. The potential of this system is given by Eqs. (5) and (6) as

$$V(r,z) = V_0\left(r^2 z - \frac{2}{3}z^3\right) + \frac{1}{\pi}\int_{-R}^{R} du \left(\frac{1}{\sqrt{(z-d+iu)^2+r^2}} - \frac{1}{\sqrt{(z+d+iu)^2+r^2}}\right) f^{(0)}(u), \tag{16}$$

where $0 \leq z < \infty$. The radius R is determined from the total charge Q by Eq. (9):

$$Q = \frac{1}{\pi}\int_{-R}^{R} du\, f^{(0)}(u). \tag{17}$$

$f^{(0)}(u)$ is the charge density on the disk and satisfies

$$f^{(0)}(u) - \frac{1}{\pi}\int_{-R}^{R} du' \frac{2d}{(2d)^2+(u-u')^2} f^{(0)}(u') = C^{(0)} + \frac{2}{3}V_0 d^3 - 2V_0 d u^2, \tag{18}$$

where $C^{(0)}$ is the value of the potential (16) on the disk at $z = d$.

Let us now find the form of the NS5-brane limit. First, note that the boundary condition at $z = d$ of Eq. (16) does not agree with that of Eq. (12): the value of the former is $C^{(0)}$, while the latter vanishes. To resolve this discrepancy, we add $-C^{(0)}z/d$ to Eq. (16). This addition of the linear term in z is justified because it does not change the supergravity solution (1). In other words, $V(r,z) - C^{(0)}z/d$ satisfies all the requirements for the electrostatic potential for PWMM: it is an axisymmetric solution to the Laplace equation and vanishes at $z = 0$. Then, the shifted potential can be expanded in Fourier series as

$$V(r,z) - \frac{C^{(0)}}{d}z = \sum_{n=1}^{\infty} c_n I_0\left(\frac{\pi n r}{d}\right)\sin\frac{\pi n z}{d}, \tag{19}$$

where c_n are Fourier coefficients. Note that the potential (12) of the electrostatic system for LST appears as the lowest Fourier mode in the expansion (19). Hence, the NS5-brane limit is given by the limit under which only c_1 survives while the other c_n vanish. From Eq. (19) with $r = R$, one can evaluate c_n as

$$c_n = \left(I_0\left(\frac{\pi n R}{d}\right)\right)^{-1}\frac{2}{d}\int_0^d dz \left\{V(R,z) - \frac{C^{(0)}}{d}z\right\}\sin\frac{\pi n z}{d}. \tag{20}$$

The leading part of the integral in Eq. (20) for large R was evaluated in Ref. [8] and found to be proportional to $V_0 R d^3$. Then, by noting that $(I_0(z))^{-1} \sim \sqrt{2\pi z}e^{-z}$ when $z \to \infty$, one finds that c_n behaves as $c_n \sim V_0 (Rd)^{3/2} e^{-n\pi R/d}$ when $R \to \infty$. Therefore, we finally obtain the NS5-brane limit as

$$R \to \infty, \quad V_0 \to \infty \quad \text{with} \quad \frac{e^{\pi R/d}}{V_0 (Rd)^{3/2}} : \text{fixed}, \tag{21}$$

where the fixed quantity is proportional to g_0 in Eq. (12).

For later use, let us express the relationship (17) between Q and R more explicitly. In the limit $R \to \infty$, one can solve the integral equation (18) as

$$f^{(0)}(u) = \frac{V_0 R^3}{3} \left\{ 1 - \left(\frac{u}{R} \right)^2 \right\}^{\frac{3}{2}}. \tag{22}$$

The derivation is given in Appendix A. Substituting this into Eq. (17), one obtains

$$Q = \frac{V_0 R^4}{8}. \tag{23}$$

This relation shows that the electric charge Q goes to infinity in the NS5-brane limit. Since Q is proportional to the D2-brane charge by Eq. (4), the D2-brane charge also goes to infinity in this limit.

3.2. *NS5-brane limit for general vacua*

Next, let us investigate the NS5-brane limit for a general vacuum of LST. The electrostatic system for the general vacuum of LST consists of Λ conducting disks between two infinite conducting plates in the presence of the background potential (12) (see Fig. 2). The net electrostatic potential is given by Eq. (13). We will show that this electrostatic system can be obtained as a double scaling limit of that for PWMM with $\Lambda + 1$ conducting disks (Fig. 1). We will find that the limit is given by

$$R_{\Lambda+1} \to \infty, \quad V_0 \to \infty \quad \text{with} \quad \frac{e^{\pi R_{\Lambda+1}/d_{\Lambda+1}}}{V_0 (R_{\Lambda+1} d_{\Lambda+1})^{3/2}} : \text{fixed}, \tag{24}$$

where $R_{\Lambda+1}$ and $d_{\Lambda+1}$ are the radius and the z-coordinate of the highest disk, respectively. This limit is a natural generalization of the NS5-brane limit (21) in the previous subsection. Hereafter, to simplify the notation, we denote the radius, the z-coordinate, and the charge of the highest disk just by R, d, and Q, respectively, instead of $R_{\Lambda+1}$, $d_{\Lambda+1}$, and $Q_{\Lambda+1}$.

Let us first focus on the $(\Lambda + 1)$th disk with charge Q, which should become infinitely large in the NS5-brane limit. The potential generated by this disk is given by

$$V_{\Lambda+1}(r, z) = \frac{1}{\pi} \int_{-R}^{R} du \left(\frac{1}{\sqrt{(z - d + iu)^2 + r^2}} - \frac{1}{\sqrt{(z + d + iu)^2 + r^2}} \right) f_{\Lambda+1}(u), \tag{25}$$

where $f_{\Lambda+1}(u)$ is the charge density of the highest disk, which is determined by Eq. (10). The radius R is related to the charge Q through Eq. (10) and

$$Q = \frac{1}{\pi} \int_{-R}^{R} du\, f_{\Lambda+1}(u). \tag{26}$$

What we expect in the case of general vacua is that the potential (25) can be divided into two parts: one of them contributes to the background part in Eq. (13) in the double scaling limit, and the other contributes to the rest. This separation should appear as a result of decomposition of the charge density $f_{\Lambda+1}(u)$ as

$$f_{\Lambda+1}(u) = f^{(0)}(u) + g(u), \tag{27}$$

where $f^{(0)}(u)$ is the charge density in the case of $\Lambda = 0$, which satisfies the same equation as Eq. (18). We set the support of $f^{(0)}(u)$ to be the same as that of $f_{\Lambda+1}(u)$, i.e., $[-R, R]$, so that the charge $\frac{1}{\pi} \int_{-R}^{R} du\, f^{(0)}(u)$ is different from Q in Eq. (26), instead. We assume that the charge associated with $f^{(0)}(u)$ is of the same order as Q when Q is large. Meanwhile, $g(u)$ corresponds to the fluctuation created by the presence of the other disks and has support on $[-R, R]$. Note that, since $g(u)$ is vanishing as $Q_s \to 0$ for any s, the ratio $g(u)/f^{(0)}(u)$ should be on the order of

$\frac{Q_s}{Q}$ for large Q. With the decomposition (27), the argument in the previous subsection ensures that the potential generated by $f^{(0)}(u)$ plus the background part (16) produces the background potential for LST in Eq. (12), in the NS5-brane limit (24).

We then show that $g(u)$ corresponds to the infinitely many mirror images in the potential (13) for LST. Note first that $g(u)$ satisfies

$$g(u) - K_{\Lambda+1}(2d)g(u) - \sum_{t=1}^{\Lambda}(K_t(d+d_t) - K_t(d-d_t))f_t(u) = C_{\Lambda+1} - C^{(0)} \tag{28}$$

for $|u| < R$, which follows from Eqs. (10) and (18). Using Eqs. (27) and (28), we find that each term on the right-hand side of Eq. (25) can be rewritten as

$$\begin{aligned}
&\int_{-R}^{R} du \frac{f_{\Lambda+1}(u)}{\sqrt{(z \mp d + iu)^2 + r^2}} \\
&= \int_{-R}^{R} du \frac{f^{(0)}(u)}{\sqrt{(z \mp d + iu)^2 + r^2}} \pm \sum_{n=1}^{\infty}\sum_{s=1}^{\Lambda} \int_{-R_s}^{R_s} du \left(\frac{f_s(u)}{\sqrt{(z - d_s \mp 2nd + iu)^2 + r^2}} \right. \\
&\left. - \frac{f_s(u)}{\sqrt{(z + d_s \mp 2nd + iu)^2 + r^2}} \right).
\end{aligned} \tag{29}$$

The derivation is shown in Appendix B. Then, from Eqs. (25) and (29), we obtain

$$V_{\Lambda+1}(r,z) = V^{(0)}(r,z) + \sum_{\substack{n=-\infty \\ \neq 0}}^{\infty} \sum_{s=1}^{\Lambda} V_{s,n}(r,z), \tag{30}$$

where

$$\begin{aligned}
V^{(0)}(r,z) &= \frac{1}{\pi} \int_{-R}^{R} du \left(\frac{1}{\sqrt{(z-d+iu)^2 + r^2}} - \frac{1}{\sqrt{(z+d+iu)^2 + r^2}} \right) f^{(0)}(u), \\
V_{s,n}(r,z) &= \frac{1}{\pi} \int_{-R_s}^{R_s} du \left(\frac{1}{\sqrt{(z-d_s-2nd+iu)^2 + r^2}} - \frac{1}{\sqrt{(z+d_s-2nd+iu)^2 + r^2}} \right) f_s(u).
\end{aligned}$$

Combined with the contributions from the other disks, $V_s(r,z)(= V_{s,0}(r,z))\,(s = 1,\ldots,\Lambda)$, and the background potential for PWMM, in the NS5-brane limit, the total electrostatic potential becomes

$$V(r,z) = V_0 \left(r^2 z - \frac{2}{3} z^3 \right) + V^{(0)}(r,z) + \sum_{n=-\infty}^{\infty} \sum_{s=1}^{\Lambda} V_{s,n}(r,z). \tag{31}$$

In the limit (24), the first two terms on the right-hand side become the background potential for LST (12) with g_0 proportional to the fixed quantity in Eq. (24). Thus, Eq. (31) indeed coincides with the electrostatic potential for a general vacuum of LST (13). Since the potential of the electrostatic system for PWMM becomes completely equivalent to that of LST as a result of the limit (24), this double scaling limit is indeed the NS5-brane limit, as desired.

We can also understand the NS5-brane limit (24) from the action of the electrostatic systems. The action of the electrostatic system for PWMM[4] is as follows:

$$S_{\rm es} = \int_{-\infty}^{\infty} dz \int_0^{\infty} 2\pi r dr \Bigg(\frac{1}{8\pi} \nabla V(r,z) \cdot \nabla V(r,z) - \sum_{s=1}^{\Lambda+1} \sigma_s(r)(\delta(z-d_s) - \delta(z+d_s)) V(r,z) \Bigg) + 2 \sum_{s=1}^{\Lambda+1} C_s \left(\int_0^{\infty} 2\pi r dr\, \sigma_s(r) - Q_s \right). \tag{32}$$

Here, the charge densities are given by $\sigma_s(r)(\delta(z-d_s) - \delta(z+d_s))$, where the second term comes from the mirror images. The coefficients C_s in Eq. (32) play the role of the Lagrange multipliers for the condition that the total charge of the sth disk is Q_s. The equation of motion for σ_s gives the condition that the potential on the sth disk is constant and is equal to C_s. In Appendix C, we show that the action (32) reduces to the action for LST in the NS5-brane limit (24). This gives more support for Eq. (24).

4. NS5-brane limit in PWMM

In this section, we consider the gauge theory side. We first review the emergent bubbling geometry from PWMM [14,15]. Then, we show that the NS5-brane limit, which we found from the gravity side in the last section, also exists at least in the planar part of a quarter-BPS sector of PWMM. In showing this, we express Eq. (24) in terms of the parameters in PWMM.

4.1. *The plane wave matrix model*

The action of PWMM in the Euclidean signature is given by

$$S = \frac{1}{g^2} \int d\tau\, {\rm Tr} \Big(\frac{1}{4} F_{MN} F^{MN} + \frac{m^2}{2} X_m X^m + \frac{i}{2} \Psi \Gamma^M D_M \Psi \Big). \tag{33}$$

We use the same notation as in Refs. [14,15]. The indices M, N run from 1 to 10. They are decomposed as $M = (1, a, m)$, where a runs from 2 to 4 and m runs from 5 to 10. F_{MN} and $D_M \Psi$ are given by

$$\begin{aligned} &F_{1M} = D_1 X_M = \partial_1 X_M - i[X_1, X_M] \ \ (M \neq 1), \\ &F_{ab} = m \epsilon_{abc} X_c - i[X_a, X_b], \quad F_{am} = -i[X_a, X_m], \quad F_{mn} = -i[X_m, X_n], \\ &D_1 \Psi = \partial_1 \Psi - i[X_1, \Psi], \quad D_a \Psi = \frac{m}{8} \epsilon_{abc} \Gamma^{bc} \Psi - i[X_a, \Psi], \quad D_m \Psi = -i[X_m, \Psi]. \end{aligned} \tag{34}$$

∂_1 is the derivative with respect to τ and X_1 is the 1D gauge field. Throughout this paper, the mass parameter m is set to 2, without loss of generality.

PWMM has $SU(2|4)$ symmetry. The vacua of PWMM are given by fuzzy spheres, which preserve the entire $SU(2|4)$ symmetry and are labeled by the $SU(2)$ representations. The vacuum configuration is given by $X_m = 0$ and

$$X_a = -2L_a = -2 \bigoplus_{s=1}^{\Lambda+1} \mathbf{1}_{N_2^{(s)}} \otimes L_a^{[D_s]} \qquad (a = 2, 3, 4), \tag{35}$$

[4]Strictly speaking, this is not an action but the minus of the potential energy with some Lagrange multipliers. However, for static configuration, they are equivalent to each other up to the volume factor of the time direction.

where Λ, $N_2^{(s)}$, and D_s are integers and $L_a^{[D]}$ stands for the $SU(2)$ generators in the D-dimensional irreducible representation. They satisfy $[L_a^{[D]}, L_b^{[D]}] = i\epsilon_{abc}L_c^{[D]}$. The matrix size of PWMM is given by $\sum_{s=1}^{\Lambda+1} N_2^{(s)} D_s$. The right-hand side of Eq. (35) is just the irreducible decomposition of a general reducible representation.

The parameters labeling the vacua are the multiplicities and dimensions of irreducible representations, $\{N_2^{(s)}, D_s\}_{s=1,\dots,\Lambda+1}$. Note that we have already used the same names for variables on the gravity side. We used $N_2^{(s)}$ for the D2-brane charges and D_s for the position of the disks, which is related to the NS5-brane charges. This usage is justified since these variables can be indeed identified with each other through the gauge/gravity correspondence. The identification for $N_2^{(s)}$ is easily understood because it corresponds to the number of fuzzy spheres in the vacuum (35), so that it should be equal to the D2-brane charges. The identification for D_s can be understood as follows. The UV region of the gravity solution (1) becomes the D0-brane solution, where the D0-brane charge is proportional to the dipole moment, $2\sum_s D_s Q_s$, generated by the conducting disks and mirror images. From the above identification of the D2-brane charges and the fact that the D0-brane charge is equal to the matrix size of PWMM, one finds that D_s corresponds to the dimensions of the irreducible representations[5]. For each theory around a vacuum labeled by $\{N_2^{(s)}, D_s\}_{s=1,\dots,\Lambda+1}$, the dual geometry on the gravity side is given by the Lin–Maldacena geometry with the same parameters.

4.2. *Emergent geometries*

If the gauge/gravity correspondence holds true, the dual geometry should be somehow realized in the strong coupling limit of PWMM. In order to see the emergence of the dual geometry, we apply the localization method, which makes exact calculations possible for some supersymmetric sectors [20].

We first choose an appropriate BPS sector. Note that the emergence of S^2 and S^5 in the geometry (1) is rather trivial because any vacua of PWMM preserve $SO(3) \times SO(6)$ symmetry. So the only non-trivial part is the emergence of the space parametrized by r and z. It was found that the vacuum expectation values (VEVs) of operators made of the complex scalar field

$$\phi(\tau) = -X_4(\tau) + X_9(\tau)\sinh\tau + iX_{10}(\tau)\cosh\tau \tag{36}$$

describe the r- and z-directions[6] [14,15]. This can be seen as follows. If we make a Wick-rotation to go back to the Lorentzian signature, the real and imaginary parts of ϕ at each fixed time are given by an $SO(3)$ scalar and an $SO(6)$ scalar, respectively, up to an $SO(2)$ ($\subset SO(6)$) rotation. So this field corresponds to a point on $S^2 \times S^5$ in the dual geometry and thus corresponds to the perpendicular directions, i.e., the space of r and z. On the other hand, when the X_{10} direction is further Wick-rotated while the time is kept Euclidean, the field (36) is shown to preserve a quarter of the whole supersymmetry and the vacuum expectation value of any operators made only of this field can be computed by the localization method.

[5]This identification can also be understood from the M-theoretic point of view. By comparing the mass spectra of PWMM and of a spherical M5-brane in the supergravity approximation, it was argued that a general vacuum of PWMM corresponds to a state with 5-branes, where the number of 5-branes is given by the dimension of the largest irreducible representation [12]. This relation is consistent with the identification for D_s, which states that $D_{\Lambda+1}$ is indeed given by the sum over all 5-brane charges.

[6]By taking VEVs, one obtains the $SO(3) \times SO(6)$ invariant part of ϕ, which should contain the information on the r- and z-directions.

The localization computation for the partition function and the VEV of such operators was done in Ref. [21]. Let us review this computation. One first needs to impose a boundary condition to define the theory as the time direction of PWMM is not compact. A natural condition for the theory around a fixed vacuum is that all fields approach the vacuum configuration as $\tau \to \pm\infty$. After imposing this condition so that the theory is defined appropriately, one adds a Q-exact term to the action, where Q stands for a supersymmetry transformation that keeps ϕ invariant. Then, from the standard argument of the localization computation [20], one-loop calculations around the saddle point of the Q-exact term give an exact result. At the saddle point, all fields except X_{10} take the vacuum configuration while there are non-trivial moduli for X_{10}. The saddle point configuration is written as

$$X_a(\tau) = -2L_a \qquad (a = 2, 3, 4), \qquad X_{10}(\tau) = \frac{M}{\cosh\tau}, \tag{37}$$

where all the other fields are vanishing at the saddle point. M is a constant Hermitian matrix commuting with L_a. When L_a are decomposed as in the right-hand side of Eq. (35), M can be decomposed as $M = \bigoplus_{s=1}^{\Lambda+1} M_s \otimes \mathbf{1}_{D_s}$, where M_s is an $N_2^{(s)} \times N_2^{(s)}$ Hermitian matrix. After calculating the one-loop determinant around the saddle point (37), one obtains the following form for the partition function [21]:

$$Z_{\mathcal{R}} = \int \prod_{s=1}^{\Lambda+1} \prod_{i=1}^{N_2^{(s)}} dm_{si}\, Z_{\text{1-loop}}(\mathcal{R}, \{m_{si}\})\, e^{-\frac{2}{g^2}\sum_s \sum_i D_s m_{si}^2}, \tag{38}$$

where $\mathcal{R}$ stands for the representation of Eq. (35) labeled by $\{N_2^{(s)}, D_s\}_{s=1,\ldots,\Lambda+1}$ and m_{si} are eigenvalues of M_s. $Z_{\text{1-loop}}(\mathcal{R}, \{m_{si}\})$ is the one-loop determinant around the saddle point given by

$$Z_{\text{1-loop}} = \prod_{s,t=1}^{\Lambda+1} \prod_{J} \prod_{i=1}^{N_2^{(s)}} \prod_{j=1}^{N_2^{(t)}}{}' \left[\frac{\{(2J+2)^2 + (m_{si} - m_{tj})^2\}\{(2J)^2 + (m_{si} - m_{tj})^2\}}{\{(2J+1)^2 + (m_{si} - m_{tj})^2\}^2} \right]^{\frac{1}{2}}. \tag{39}$$

Here J runs from $|D_s - D_t|/2$ to $(D_s + D_t)/2 - 1$. We denote by $\prod'$ the product in which the second factor in the numerator with $s = t$, $J = 0$, and $i = j$ is not included. Then, any operator in the BPS sector, which is made only of ϕ, can be computed by the partition function (38); namely, the VEV of a function of ϕ, say $f(\phi)$, is computed as

$$\langle f(\phi) \rangle = \langle f(-2L_4 + iM) \rangle_M, \tag{40}$$

where $\langle \cdots \rangle_M$ stands for the expectation value with respect to the partition function (38).

The partition function (38) describes the quarter-BPS sector of the theory around the vacuum labeled by the representation $\mathcal{R}$. Insertions of operators of ϕ correspond to the quarter-BPS fluctuations around the vacuum. On the supergravity side, they will correspond to the fluctuations of fields that preserve the same supersymmetry. On the other hand, if there is no insertion of the operators, the partition function (38) is dominated by the vacuum configuration, which should contain the information on the background geometry of the dual string theory. If we can solve the model (38) completely, we can check whether these correspondences are true or not. Though solving this model for arbitrary parameters is very difficult, the problem is simplified in the large-N limit, where the eigenvalue integral can be evaluated by the saddle point approximation. This is also the regime where the supergravity approximation becomes valid.

An appropriate parameter region to see the correspondence is given as follows [14,15]. In order to suppress the bulk string coupling correction, we take the 't Hooft limit

$$N_2^{(s)} \to \infty, \quad \lambda^{(s)} = g^2 N_2^{(s)} = \text{fixed}. \tag{41}$$

Moreover, to suppress the α'-corrections, we consider the region where

$$N_5^{(s)} = D_s - D_{s-1} \gg 1, \quad \lambda^{(s)} \gg D_s, \tag{42}$$

for arbitrary s. In this parameter region, the effective action of Eq. (38) is given by

$$\begin{aligned} S_{\text{eff}} = &\sum_{s=1}^{\Lambda+1} \frac{2D_s}{g^2} \int dx\, x^2 \rho^{(s)}(x) + \sum_{s=1}^{\Lambda+1} \frac{\pi}{2} \int dx\, \rho^{(s)}(x)^2 \\ &- \sum_{s,t=1}^{\Lambda+1} \frac{1}{2} \int dxdy \left[\frac{D_s + D_t}{(D_s + D_t)^2 + (x-y)^2} - \frac{|D_s - D_t|}{(D_s - D_t)^2 + (x-y)^2} \right] \rho^{(s)}(x) \rho^{(t)}(y) \\ &- \sum_{s=1}^{\Lambda+1} \mu_s \left(\int dx\, \rho^{(s)}(x) - N_2^{(s)} \right), \end{aligned} \tag{43}$$

where $\rho^{(s)}(x)$ is the eigenvalue distribution, $\rho^{(s)}(x) = \sum_{i=1}^{N_2^{(s)}} \delta(x - m_{si})$, and μ_s is the Lagrange multiplier imposing the normalization for $\rho^{(s)}(x)$:

$$N_2^{(s)} = \int_{-x_m^{(s)}}^{x_m^{(s)}} dx\, \rho^{(s)}(x). \tag{44}$$

$x_m^{(s)}$ is the extent of the support of $\rho^{(s)}(x)$. In the 't Hooft limit, the saddle point approximation for the variables $\rho^{(s)}$ becomes exact and the theory becomes basically a classical theory with the action (43).

Let us now show that this classical theory is equivalent to the axially symmetric electrostatic system considered on the gravity side. Below, we verify this equivalence[7] by comparing the electrostatic action (32) and the quarter-BPS effective action (43).

Back on the gravity side, we first rewrite the electrostatic action (32) in terms of the charge densities $f_s(u)$. By using Eqs. (5) and (7), one can show that the potential V_s satisfies the following relations[8]:

$$\begin{aligned} &\int_{-\infty}^{\infty} dz \int_0^{\infty} rdr\, V_s(r,z) \triangle V_t(r,z) \\ &\quad = \frac{4}{\pi^2} \left(\int_{-\infty}^{\infty} dudu' \frac{|d_s + d_t|}{(d_s + d_t)^2 + (u-u')^2} f_s(u) f_t(u') \right. \\ &\quad \left. - \int_{-\infty}^{\infty} dudu' \frac{|d_s - d_t|}{(d_s - d_t)^2 + (u-u')^2} f_s(u) f_t(u') \right) \quad (t \neq s), \end{aligned} \tag{45}$$

$$\begin{aligned} &\int_{-\infty}^{\infty} dz \int_0^{\infty} rdr\, V_s(r,z) \triangle V_s(r,z) \\ &\quad = \frac{4}{\pi^2} \left(\int_{-\infty}^{\infty} dudu' \frac{2d_s}{(2d_s)^2 + (u-u')^2} f_s(u) f_s(u') - \pi \int_{-\infty}^{\infty} du f_s(u)^2 \right), \end{aligned} \tag{46}$$

[7] This equivalence was originally argued by using the equations of motion in Refs. [14,15].

[8] It is convenient to use the following expression for $V(r,z)$:

$$V_s(r,z) = 4\pi \int dz' r' dr'\, G(r,z;r',z') \sigma_s(r') (\delta(z' + d_s) - \delta(z' - d_s)).$$

Here,

$$G(r,z;r',z') = -\frac{1}{2} \int_0^{\infty} du\, e^{-u|z-z'|} J_0(ru) J_0(r'u)$$

is the Green function of the Laplacian in the cylindrical coordinate, where J_0 is the Bessel function of the 0th order.

$$\int_{-\infty}^{\infty} dz \int_0^{\infty} rdr\,(r^2 z - \frac{2}{3}z^3) \triangle V_s(r,z) = \frac{4}{\pi}\int_{-1}^{1} du \left(-2d_s u^2 + \frac{2d_s^3}{3}\right) f_s(u). \tag{47}$$

By using these relations, we can rewrite Eq. (32) as

$$\begin{aligned} S_{\rm es} = -\frac{2}{\pi}\Bigg[& \sum_{s=1}^{\Lambda+1} 2V_0 d_s \int_{-R_s}^{R_s} du\, u^2 f_s(u) + \sum_{s=1}^{\Lambda+1}\frac{1}{2}\int du\, f_s(u)^2 \\ & - \sum_{s,t=1}^{\Lambda+1}\frac{1}{2\pi}\int du du' \left[\frac{d_s+d_t}{(d_s+d_t)^2+(u-u')^2} - \frac{|d_s-d_t|}{(d_s-d_t)^2+(u-u')^2}\right] f_s(u) f_t(u') \\ & - \sum_{s=1}^{\Lambda+1}(C_s + \frac{2}{3}V_0 d_s^3)\left(\int du\, f_s(u) - \pi Q_s\right)\Bigg], \end{aligned} \tag{48}$$

where we have neglected total derivatives and terms that contain no dynamical variables.

Comparing the gauge theory side (43) and the gravity side (48), we find the equivalence relation

$$S_{\rm es} = -\frac{\pi^3}{16} S_{\rm eff} \tag{49}$$

under the identifications

$$\frac{1}{g^2} = \frac{\pi^2}{2} V_0, \tag{50}$$

$$\rho^{(s)}(x) = \frac{4}{\pi^2} f_s\left(\frac{\pi}{2}x\right), \tag{51}$$

$$x_m^{(s)} = \frac{2}{\pi} R_s, \tag{52}$$

$$\mu_s = \frac{4}{\pi}\left(C_s + \frac{2}{3}V_0 d_s^3\right). \tag{53}$$

Therefore, $S_{\rm es}$ and $S_{\rm eff}$ are equivalent up to irrelevant constant terms and total derivatives, and thus give the same extremum. Some consistency checks of this identification can be found in Refs. [14,15]. It turns out from Eq. (51) that the sth eigenvalue distribution $\rho^{(s)}(x)$ in PWMM is equivalent to the charge density on the sth disk in the dual gravity. Note that the charge density fully determines the geometry once the gravity solution is in the form of Eq. (1) with the Laplace equation (2) and the positivity and regularity conditions. In this sense, one can say that the dual geometry is formed by the eigenvalue distribution of the scalar fields in PWMM, through the relation (51). Therefore, this provides a glimpse into a manifestation of geometry from PWMM.

4.3. *The double scaling limit in PWMM*

The equivalence (49) clearly shows that the planar part of the quarter-BPS sector of PWMM has the same NS5-brane limit as the gravity side discussed in Sect. 3. In this subsection, we rewrite the NS5-brane limit (24) using the parameters on the gauge theory side: $D := D_{\Lambda+1}$, $N_2 := N_2^{(\Lambda+1)}$, and g.

To do this, we have to rewrite d ($=d_{\Lambda+1}$), R ($=R_{\Lambda+1}$), and V_0 in Eq. (24) in terms of the quantities in PWMM. It is already shown that d and V_0 are given in terms of D and g^2, respectively, in Eqs. (4) and (50), whereas R is given by the upper edge of the support ($x_m^{(\Lambda+1)}$ in Eq. (52)) of the eigenvalue density $\rho^{(\Lambda+1)}(x)$. Below, we will partly solve the saddle point

equations for the eigenvalue densities and express $x_m^{(\Lambda+1)}$ explicitly in terms of the parameters of PWMM.

The saddle point equation of $\rho^{(s)}(x)$ is obtained from Eq. (43) as

$$\mu_s = \frac{2D_s}{g^2}x^2 + \pi\rho^{(s)}(x) - \frac{i}{2}\sum_{t=1}^{\Lambda+1}\Big\{\big(\omega^{(t)}(x+i(D_s+D_t)) - \omega^{(t)}(x-i(D_s+D_t))\big) - \big(\omega^{(t)}(x+i|D_s-D_t|) - \omega^{(t)}(x-i|D_s-D_t|)\big)\Big\}, \tag{54}$$

where $\omega^{(t)}(z)$ are the resolvents for each eigenvalue density, $\omega^{(t)}(z) := \int dx\,\rho^{(t)}(x)/(z-x)$. $\rho^{(t)}(x)$ is obtained from $\omega^{(t)}(z)$ via $\rho^{(t)}(x) = -\frac{1}{2\pi}(\omega^{(t)}(x+i0) - \omega^{(t)}(x-i0))$. Now, let us consider the saddle point equations for $\rho^{(\Lambda+1)}(x)$ in the NS5-brane limit (24). In terms of D_s and $x_m^{(\Lambda+1)}$, the limit implies $x_m^{(\Lambda+1)} \gg D_s$. Then, the typical scale of the eigenvalue density $\rho^{(\Lambda+1)}(x)$ is naturally expected as $|x| \sim x_m^{(\Lambda+1)} \gg D_s$. In this regime, the saddle point equations (54) are reduced to a much simpler form:

$$\mu_s = \frac{2D_s}{g^2}x^2 + \left(D_s\sum_{t\geq s} + \sum_{t<s}D_t\right)\big(\omega^{(t)\prime}(x+i0) + \omega^{(t)\prime}(x-i0)\big). \tag{55}$$

From the equations for $s = \Lambda$ and $\Lambda+1$, one obtains the relation

$$\bar{\mu} - \frac{2}{g^2}x^2 = \omega^{(\Lambda+1)\prime}(x+i0) + \omega^{(\Lambda+1)\prime}(x-i0), \tag{56}$$

where $\bar{\mu} = (\mu_{\Lambda+1} - \mu_\Lambda)/N_5^{(\Lambda+1)}$. As shown in Appendix A, integrating Eq. (56) over x yields the saddle point equation for a well-known quartic matrix model, which can be easily solved. As a result, the eigenvalue density for $\omega^{(\Lambda+1)}(z)$ is obtained as

$$\rho(x) = \frac{x_m}{2\pi}\left(\bar{\mu} - \frac{2x_m^2}{3g^2}\left(\frac{1}{2} + \frac{x^2}{x_m^2}\right)\right)\left(1 - \left(\frac{x}{x_m}\right)^2\right)^{\frac{1}{2}}, \tag{57}$$

where $\rho(x) = \rho^{(\Lambda+1)}(x)$ and $x_m = x_m^{(\Lambda+1)}$. The normalization of $\rho(x)$ (44) imposes a condition among parameters:

$$\bar{\mu} = \frac{x_m^4 + 8g^2N_2}{2g^2x_m^2}. \tag{58}$$

Recall that there is one more condition for $\rho(x)$. As mentioned in Sect. 2, the finiteness of the corresponding gravity solution requires each charge density $f_s(u)$ to have a finite derivative at the edges. Imposing the same condition on $\rho(x)$ together with Eq. (58), we obtain

$$x_m^4 = 8g^2N_2. \tag{59}$$

This relation can also be derived from the purely field-theoretic viewpoint by application of the least action principle. The details of this derivation are explained in Appendix A. Then the eigenvalue density (57) becomes

$$\rho(x) = \frac{x_m^3}{3\pi g^2}\left(1 - \left(\frac{x}{x_m}\right)^2\right)^{\frac{3}{2}}. \tag{60}$$

This is exactly the same form as that for $\Lambda = 1$ given by Eq. (A9).

Finally, by substituting the relations (4), (50), and (59) into Eq. (24), we find that the NS5-brane limit can be written as

$$N_2 \to \infty, \quad \frac{1}{N_2}(g^2N_2)^{\frac{5}{8}}\exp\left[2^{\frac{3}{4}}\pi\frac{(g^2N_2)^{\frac{1}{4}}}{D}\right] \equiv \tilde{g}_s : \text{fixed}. \tag{61}$$

The fixed parameter $\tilde{g}_s$ corresponds to g_0 in Eq. (12) on the gravity side, and hence it is argued in Ref. [8] that $\tilde{g}_s$ is considered as an effective coupling of the IIA LST.

At finite N_2, there are possible non-planar corrections to the quantities (51)–(53), which could correct the fixed parameter in expression (61). However, we claim that the double scaling limit (61) should be valid with the non-planar corrections taken into account. Obviously, the correction appears when the ratio of the correction $\delta\tilde{g}_s$ to the original $\tilde{g}_s$ approaches a finite value or infinity in the double scaling limit (61). In the former case, each g-dependent coefficient in the non-planar corrections appears such that the coefficient combines with $1/N_2$ to form $\tilde{g}_s$ in the limit. Thus, the corrected fixed parameter $\tilde{g}_s + \delta\tilde{g}_s$ becomes a polynomial in $\tilde{g}_s$, and one can still fix $\tilde{g}_s$ for the double scaling limit. The latter case should be impossible if the gauge/gravity duality holds because the perturbative expansion in terms of quantum correction breaks down otherwise. Therefore, the double scaling limit should remain unchanged by the non-planar corrections.

5. Numerical results

In this section, we show our numerical results for the quarter-BPS sector in PWMM and discuss the existence of the double scaling limit. We employ the hybrid Monte Carlo method to perform the integration in the partition function (38), which is the effective theory of the quarter-BPS sector. Since the numerical results provide information on N_2-dependence, one can discuss not only the existence of the double scaling limit but also the quantum loop correction, which is interpreted as a $\tilde{g}_s$ correction in the LST as we will see below.

5.1. *Expansion with respect to the LST coupling*

The double scaling limit (61) is understood as the limit that captures all orders in the genus expansion even if N_2 goes to infinity [8,14]. Since PWMM in this BPS sector is expressed by the matrix integral (38), the VEV of a quarter-BPS operator can be expanded in powers of $1/N_2$ as

$$\langle \mathcal{O} \rangle_M = \sum_{n=0}^{\infty} d_n(\lambda) N_2^{-n}, \tag{62}$$

where $\lambda = g^2 N_2$ and $\mathcal{O}$ is a quantity equivalent to the quarter-BPS operator, which is thus made of M. As discussed in the previous section, PWMM realizes the IIA LST on S^5 in the NS5-brane limit (61), which naturally suggests that the VEV is expanded with respect to the effective LST coupling $\tilde{g}_s$. Hence, the expansion (62) is rewritten as

$$\langle \mathcal{O} \rangle_M = C(\lambda) \sum_{n=0}^{\infty} c_n \tilde{g}_s^n, \tag{63}$$

where $C(\lambda)$ is an overall factor, which may be, in general, infinitely large in the limit. The coefficients c_n are supposed to be independent of λ because any LST observable is considered as a finite function of $\tilde{g}_s$ up to the overall factor. Therefore, if the NS5-brane limit (61) successfully realizes IIA LST, we will observe that the ratios $d_{n+1}(\lambda)/d_n(\lambda)$ have the following λ-dependence:

$$\frac{d_{n+1}(\lambda)}{d_n(\lambda)} = \frac{c_{n+1}}{c_n} \lambda^{\frac{5}{8}} \exp\left[2^{\frac{3}{4}} \pi \frac{\lambda^{\frac{1}{4}}}{D} \right], \tag{64}$$

for each n. This is a non-trivial prediction, which we examine in the next subsection.

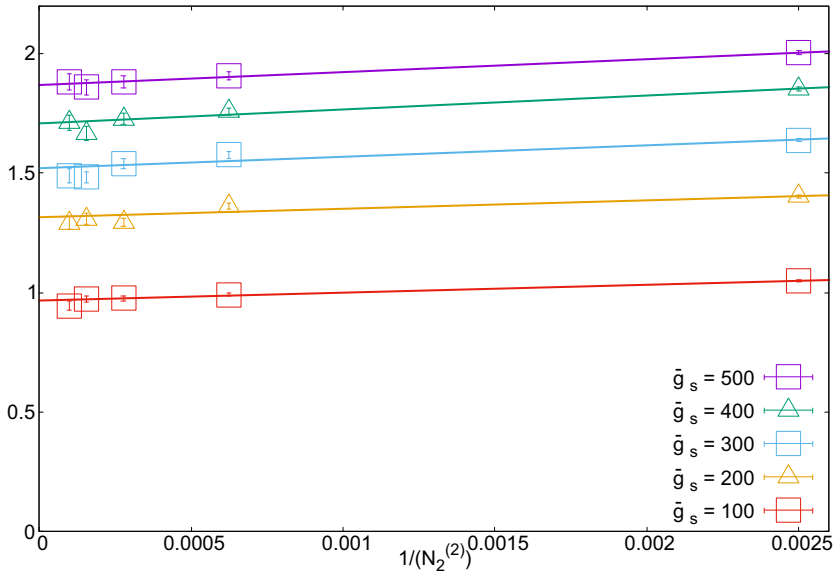

Fig. 3. N_2-dependence of $\langle \mathrm{Tr} M_1^2 \rangle_M$ for fixed values of $\tilde{g}_s$. Each set of data points for a fixed $\tilde{g}_s$ is fit by a linear function $a + b/N_2$, where a and b are fitting parameters.

5.2. *Numerical analysis*

We simulate the quarter-BPS PWMM system (38) with $\Lambda = 1$ by using the hybrid Monte Carlo method. From the viewpoint of the electrostatic system, this case corresponds to a system consisting of one conducting disk at $z = d_1$ between two larger conducting disks at $z = 0$ and d_2 in the background potential (3). While the conducting disk at $z = 0$ has an infinitely large radius, the other larger one at $z = d_2$ becomes infinitely large after the NS5-brane limit is taken.

The quarter-BPS operators that we measure are constructed of the "moduli" matrix M, which has the following structure in this case:

$$M = (M_1 \otimes \mathbf{1}_{D_1}) \oplus (M_2 \otimes \mathbf{1}_{D_2}). \tag{65}$$

In this paper, we compute $\mathrm{Tr} M_s^2$, which are projected traces onto each block matrix for $s = 1$ and 2.

In the following, we discuss two ways to see the validity of the NS5-brane limit.

5.2.1 *Finiteness in the double scaling limit of PWMM.*

One way is to compute the quantities for $s = 1$ at fixed $\tilde{g}_s$ and check whether they take finite values at large N_2 $(= N_2^{(2)})$. Since M_1 corresponds to the middle conducting disk in the electrostatic picture and therefore to a D2-brane flux in the supergravity picture, the quantities for $s = 1$ should describe a non-perturbative object in the IIA LST. Thus, if the double scaling limit exists and reproduces the IIA LST, such matrix-model quantities are expected to be finite in the limit in general. Therefore, $C(\lambda)$ in Eq. (63) should approach a finite constant for $s = 1$. The plot of $\langle \mathrm{Tr} M_1^2 \rangle_M$ is shown in Fig. 3 for $\tilde{g}_s = 100, 200, 300, 400$, and 500 (see Appendix D.1 for our choice of $N_2^{(s)}$ and D_s), the values of which are chosen so that they satisfy $\lambda \gg D^4$ in Eq. (42). One can see that they look convergent at each $\tilde{g}_s$ as N_2 tends to infinity. This supports the validity of the NS5-brane limit.

5.2.2 *Computation of c_1/c_0.*

Another way is to compute quantities with the 't Hooft coupling λ fixed and then read off the coefficients $d_n(\lambda)$ in Eq. (62) by fitting the data by a polynomial

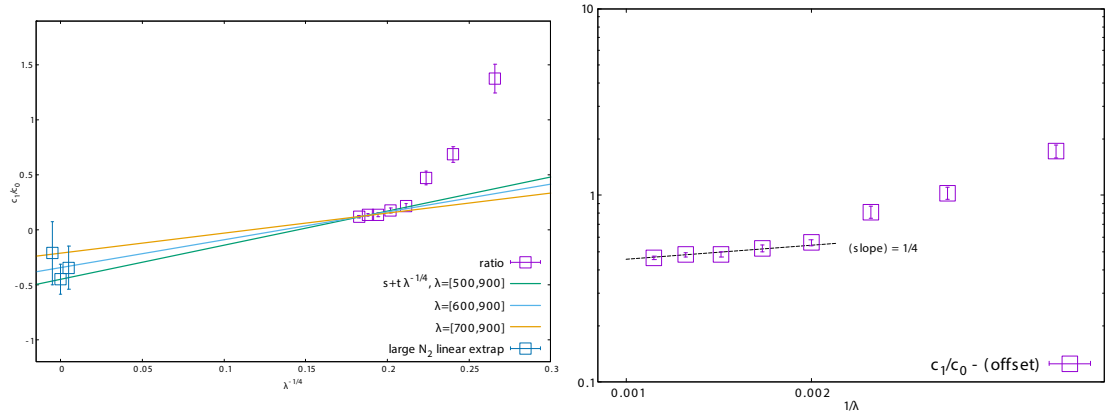

Fig. 4. Plots of the ratio c_1/c_0 for $\langle \mathrm{Tr} M_1^2 \rangle_M$. (Left) The horizontal axis is $\lambda^{-1/4}$. The green, blue, and orange lines are the fitted lines for different regions of λ, by $s + t\lambda^{-1/4}$, where s and t are fitting parameters. The blue squares just around $\lambda^{-1/4} = 0$ show the extrapolated value of c_1/c_0 by the 't Hooft limit. (Right) The horizontal axis is $1/\lambda$. The black dashed line indicates a line with slope 1/4.

function. If the ratio $d_{n+1}(\lambda)/d_n(\lambda)$ behaves as in Eq. (64) at large λ, or, equivalently, if the ratio c_{n+1}/c_n approaches a constant as λ goes to infinity, finiteness of each term in the genus expansion is guaranteed even in the NS5-brane limit. This means that the quantities have non-trivial dependence on $\tilde{g}_s$ in the computed parameter region, and therefore that a system on NS5-branes is considered to be realized in the parameter region.

The ratio c_1/c_0 at each λ is computed by fitting the numerically obtained expectation values. The expectation values are computed for several N_2, and hence the large-N_2 extrapolation through the relation (64) provides the coefficients, $d_0(\lambda)$ and $d_1(\lambda)$. See Appendix D.2 for our choice of $N_2^{(s)}$ and D_s in this computation and Appendix D.3 for $d_0(\lambda)$ and $d_1(\lambda)$ obtained by the fitting. We plot c_1/c_0 for $\mathrm{Tr} M_1^2$ at $\lambda = 200, 300, \ldots, 900$ in Fig. 4.

We fit the obtained data of c_1/c_0 by a polynomial function of $\lambda^{-\frac{1}{4}}$ in the left panel in Fig. 4. This is motivated by the gauge/gravity duality, which predicts that α'-expansion corresponds to expansion in powers of $\lambda^{-\frac{1}{4}}$ since $R_{S^5}^2/\alpha' = 2\pi(8\lambda)^{\frac{1}{4}}$ in the NS5-brane limit[9] [14]. The figure shows that the linear fits in $\lambda^{-\frac{1}{4}}$ for data with $\lambda \geq 500$, 600, and 700 are consistent with each other and that the ratio approaches $c_1/c_0 \sim -0.3$. Note that one cannot exclude the possibility that it converges to 0.

To numerically support the polynomial fitting in $\lambda^{-\frac{1}{4}}$, we fit the log–log plot of c_1/c_0 against $1/\lambda$ by a linear function with slope 1/4 in the right panel in Fig. 4. To properly detect the slope, the ratio c_1/c_0 is subtracted by an offset $s = -0.34(20)$, which is measured by the fitting $s + t\lambda^{-\frac{1}{4}}$ for $600 \leq \lambda \leq 900$. The good agreement seen in the figure reinforces the exponent $-1/4$ of λ in the fitting polynomial and suggests that the correction at large λ corresponds to the α'-correction to the NS5-brane system.

Another important check of the linear fitting is $\tilde{g}_s$-independence. Even though the coefficients c_i are supposed to be independent of $\tilde{g}_s$, numerical results of c_1/c_0 may depend on $\tilde{g}_s$ because of numerical errors that could be caused by the large values of $\tilde{g}_s$ in our parameter choice. However, setting $\tilde{g}_s$ to the order of 1 requires substantially larger N_2 than we used in the simulations. Therefore, we extrapolate the data restricted to $\tilde{g}_s \leq \tilde{g}_s^{\max}$, with some constant

[9] R_{S^5} is the S^5 radius at the spatial point corresponding to the edge of the highest conducting disk in the electrostatic picture.

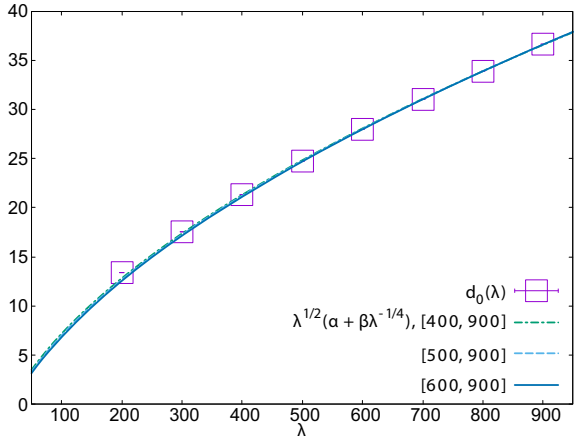

Fig. 5. A plot of $d_0(\lambda)$ for $\langle \mathrm{Tr} M_2^2 \rangle_M$ and some fits with different ranges. The curves show fitting results by $\lambda^{1/2}(\alpha + \beta\lambda^{-1/4})$ with fitting parameters α and β. We see that it is consistent with the theoretical result at large λ.

$\tilde{g}_s^{\max}$, and compare the extrapolated values of c_1/c_0 at large λ with different $\tilde{g}_s^{\max}$. We find that the extrapolation is not influenced drastically with $\tilde{g}_s^{\max}$. See Appendix D.4 for the detailed results.

In order to verify that we simulate the system at large enough λ to reproduce the physics on the NS5-branes, we check the λ-dependence of $\langle \mathrm{Tr} M_2^2 \rangle_M$. It is shown in Ref. [14] that this quantity grows as $\lambda^{\frac{1}{2}}$ at large λ, i.e., $C(\lambda) \sim \lambda^{\frac{1}{2}}$. The next-to-leading order of the quantity is naturally assumed to be the order of $\lambda^{\frac{1}{4}}$, as discussed for the fitting of c_1/c_0. We observe that the numerical results of $\langle \mathrm{Tr} M_2^2 \rangle_M$ agree with fits at large λ by $\lambda^{1/2}(\alpha + \beta\lambda^{-1/4})$ with fitting parameters α and β, shown in Fig. 5. Our data are consistent with the theoretically expected behavior; hence this supports the validity of our parameter choice.

Even though the above arguments support the linear fitting in Fig. 4 to some extent, the deviation from the linear fit does not look like a quadratic correction. However, since the 5-brane physics is not well understood yet, the exact correction to the linear term, which should correspond to higher α'-corrections, is simply not known. Thus, it is possible that some higher-order terms are accidentally large or that the fitting function is not even a polynomial but in a more complicated form. In addition, it is also a possible scenario that there is a phase transition around $\lambda = 450$, which may be caused by the large-N_2 limit (see Fig. 6).

6. Summary and discussion

We investigated a novel realization of the IIA LST on $R \times S^5$ by PWMM in a double scaling limit, which is called the NS5-brane limit throughout this paper. The IIA LST on $R \times S^5$ is known to have many discrete vacua and the theory around each vacuum is conjectured to be realized by PWMM in the limit. For the trivial vacuum, the form of the NS5-brane limit was obtained in Ref. [8], where the limit was first obtained on the gravity side and translated into field-theory language based on some reasonable arguments.

In this paper, we obtained the NS5-brane limit for general vacua. We first found the NS5-brane limit on the gravity side in terms of the electrostatic description. Then, by making use of the localization method, we showed the equivalence between the effective action of a quarter-BPS sector in PWMM and the action for the electrostatic system. This equivalence made it

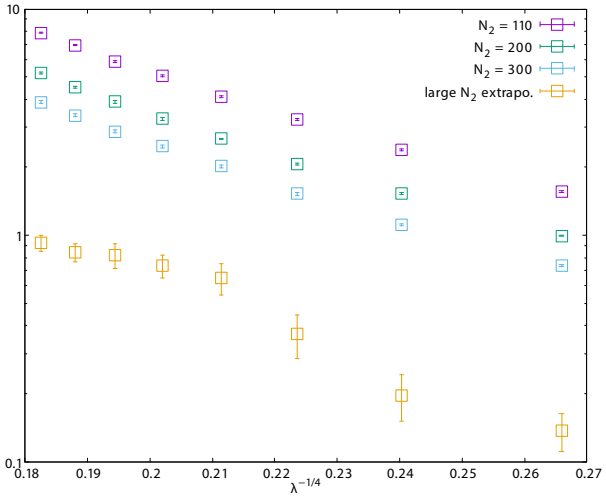

Fig. 6. A plot of $\langle \mathrm{Tr} M_1^2 \rangle_M$ against $\lambda^{-\frac{1}{4}}$. The purple, green, and blue points are numerical results with $N_2 = 100$, 200, and 300, respectively. The orange points represent extrapolated values at large N_2. Around $\lambda^{-\frac{1}{4}} = 0.22$, the behavior of the extrapolated points changes rather drastically, which may suggest that there is a phase transition.

possible to directly identify the parameters on both sides. Using this relation, we finally expressed the form of the NS5-brane limit in terms of the parameters in PWMM.

The use of the localization computation also yields a byproduct that one can see the direct equivalence between the quarter-BPS sector in PWMM and the electrostatic system on the gravity side. This equivalence assures us that the NS5-brane limit, which we found on the gravity side, also exists in the quarter-BPS sector in PWMM. However, since we took the planar limit of PWMM in deriving this equivalence, our analytical proof on the presence of the NS5-brane limit in PWMM is also limited to this sector. Note that our numerical results in Sect. 5 presented evidence of the NS5-brane limit in a more general sector beyond the planar limit.

The IIA LST around a trivial vacuum can also be obtained by different double scaling limits of the other $SU(2|4)$ symmetric theories, $\mathcal{N} = 8$ SYM on $R \times S^2$ and $\mathcal{N} = 4$ SYM on $R \times S^3/Z_k$ [13]. By applying the procedure used in this paper, it would be possible to show the existence of the double scaling limit to obtain the IIA LST around a general vacuum from these gauge theories.

In the numerical computation, we obtained results consistent with the existence of the double scaling limit. We also found that the coefficients in the $\tilde{g}_s$ expansion of $\mathrm{Tr} M_1^2$, which is associated with the electric charge density (or some sort of D2-brane charge density in the supergravity picture), satisfied $c_1/c_0 \sim -0.3$.

Our result is the first computation to obtain a $\tilde{g}_s$ correction in LST using PWMM, which can be interpreted as a quantum loop correction in the Lin–Maldacena geometry in the limit (41), to the best of our knowledge. However, the linear fitting of c_1/c_0 was not quite satisfactory. This could be due to the lack of knowledge of the 5-brane physics. In this regard, it would be interesting to clarify whether there is a phase transition in the large-N limit, inferred in Fig. 6.

Since the error is large, the ratio c_1/c_0 for $\mathrm{Tr} M_1^2$ was consistent with 0, which means that $\mathrm{Tr} M_1^2$ would be independent of $\tilde{g}_s$. If this is the case, the $\tilde{g}_s$-independence of the quantity would suggest that there is a non-renormalizable theorem, or it is equally possible that only the next-to-leading correction in $\tilde{g}_s$ is absent while higher-order corrections are present. Unfortunately,

it is not feasible to determine the higher-order terms to high precision by the current numerical method, or, at least, in the parameter region of our choice.

The relation of the obtained double scaling limit with the M-theoretic viewpoint is also interesting. In Refs. [16,17], it was revealed that, in the strong coupling limit of PWMM, the low-energy modes of the $SO(6)$ matrices form the S^5 geometry with the correct radius predicted in Ref. [12]. Even though its interpretation of the emerging geometries is slightly different from the gauge/gravity, they should be related in some way.

Acknowledgments

The work of G.I. was supported by JSPS KAKENHI Grant Number JP 19K03818. H.W. was supported in part by JSPS KAKENHI Grant Number JP 21J13014.

Funding

Open Access funding: SCOAP[3].

A. Solution in the NS5-brane limit with $\Lambda = 1$

The solution to Eq. (18) was obtained in Ref. [8]. See Ref. [14] for the gauge-theoretic viewpoint. In Ref. [8], Eq. (18) was solved by imposing the constraint that the derivative of $f^{(0)}$ is vanishing at the edges of the support of $f^{(0)}$. This comes from the finiteness of the corresponding gravity solution. Note that from the gauge-theoretic viewpoint, the meaning of this condition is not clear and it seems to be unnatural to impose the condition by hand on the corresponding matrix integral discussed in Ref. [14]. However, it turns out that, on the gauge theory side, the solution with the condition imposed is chosen by the least action principle. In this appendix, we derive the solution from the action principle, not imposing the condition.

Let us start with the action of the electrostatic system, which is given by Eq. (32) with $\Lambda = 0$:

$$\begin{aligned} S_{\text{eff}} = \frac{32}{\pi^4}\Bigg[& 2V_0 d \int_{-R}^{R} du\, u^2 f^{(0)}(u) + \frac{1}{2}\int du\, f^{(0)}(u)^2 \\ & -\frac{1}{2\pi}\int du du' \left[\frac{2d}{(2d)^2+(u-u')^2}\right] f^{(0)}(u) f^{(0)}(u') \\ & -(C^{(0)} + \frac{2}{3}V_0 d^3)\left(\int du\, f^{(0)}(u) - \pi Q\right)\Bigg]. \end{aligned} \tag{A1}$$

The saddle point equation of $f^{(0)}$ is given by Eq. (18). If we take the $d/R \to 0$ limit in Eq. (18), we obtain

$$\omega^{(0)\prime}(u - i0) + \omega^{(0)\prime}(u + i0) = \mathcal{C} - 2\pi V_0 u^2, \tag{A2}$$

where $\mathcal{C} = \frac{\pi}{d}(C^{(0)} + \frac{2}{3}V_0 d^3)$ and $\omega^{(0)}(z)$ is the resolvent:

$$\omega^{(0)}(z) = \int_{-R}^{R} du \frac{f^{(0)}(u)}{z-u}. \tag{A3}$$

If we integrate Eq. (A2) once, we obtain an equation that is equivalent to the equation of motion of the one-matrix model with a quartic interaction. Thus, we find that the solution is given in the same form as the quartic matrix model:

$$\omega^{(0)}(z) = \frac{1}{2}\left(\mathcal{C}z - \frac{2\pi V_0}{3}z^3\right) - \frac{1}{2}\left(\mathcal{C} - \frac{2\pi V_0 R^2}{3}\left(\frac{1}{2} + \frac{z^2}{R^2}\right)\right)\left(z^2 - R^2\right)^{\frac{1}{2}}. \tag{A4}$$

Furthermore, the normalization (17) gives another relation as

$$\mathcal{C} = \pi \frac{V_0 R^4 + 8Q}{2R^2}. \tag{A5}$$

By eliminating $\mathcal{C}$ using this relation, we obtain

$$f^{(0)}(u) = \frac{V_0}{3}\left(\frac{V_0 R^4 + 24Q}{4R^2 V_0} - u^2\right)\left(R^2 - u^2\right)^{\frac{1}{2}}. \tag{A6}$$

Note that the semi-positivity of $f^{(0)}(u)$ imposes the condition that $R \leq (8Q/V_0)^{\frac{1}{4}}$.

Then, we use the action principle. By substituting Eq. (A6) into Eq. (A1), we find that the R-dependence of the effective action is given by

$$S_{\text{eff}} = \frac{d}{3\pi^3 R^2}\left(192Q^2 + 48\pi V_0 Q R^2 - \pi^2 V_0^2 R^6\right). \tag{A7}$$

This has an extremum point at

$$R = \left(\frac{8Q}{V_0}\right)^{\frac{1}{4}}. \tag{A8}$$

Under the condition that $f^{(0)}(u)$ is semi-positive everywhere, we can find that this point is also the minimum of the action. Now, by substituting Eq. (A8), we obtain

$$f^{(0)}(u) = \frac{V_0 R^3}{3}\left\{1 - \left(\frac{u}{R}\right)^2\right\}^{\frac{3}{2}} = \frac{V_0}{3}\left(\sqrt{\frac{8Q}{V_0}} - u^2\right)^{\frac{3}{2}}. \tag{A9}$$

Thus, the solution with $\frac{df^{(0)}}{du}(\pm R) = 0$ is indeed obtained through the least action principle.

The same procedure can also be applied to calculating Eq. (60). The procedure is as follows. Firstly, in the NS5-brane limit, the leading behavior of $\rho(x)$ is governed only by self-interaction since the effect from the eigenvalues for $s = 1,\ldots,\Lambda$ is on the order of $\frac{Q_s}{Q}$ and hence suppressed. Then, by plugging Eqs. (57) and (58) into the effective action (43) and neglecting the interaction terms involving $\rho^{(s)}(x)$ for $s = 1,\ldots,\Lambda$, one obtains the expression of the action written by x_m in the leading of D/x_m. Finally, one finds that its minimum point is given by Eq. (59).

B. Derivation of Eq. (29)

In this appendix, we derive Eq. (29) from Eq. (28).

We first show that the right-hand side of Eq. (28), $C_{\Lambda+1} - C^{(0)}$, vanishes in the NS5-brane limit (24). For this purpose, we integrate Eq. (28) over u from $-R$ to R:

$$C_{\Lambda+1} - C^{(0)} = \frac{2d}{\pi R}\int_{-R}^{R} du\, \frac{g(u)}{R^2 - u^2} + \sum_{s=1}^{\Lambda} \frac{2d_s}{\pi R}\int_{-R_s}^{R_s} du\, \frac{f_s(u)}{R^2 - u^2} + \cdots, \tag{B1}$$

where we have used

$$\int_{-R}^{R} du\, \frac{\delta}{\delta^2 + (u-u')^2} = \pi - \frac{2R\delta}{R^2 - u'^2} + \mathcal{O}((\delta/R)^3). \tag{B2}$$

As noted below Eq. (27), $g(u)$ and $f_s(u)$ are on the order of Q_s and $g(\pm R) = 0$. Using these conditions, one can show that the right-hand side of Eq. (B1) vanishes in the NS5-brane limit. Thus, in the NS5-brane limit, $C_{\Lambda+1} - C^{(0)} \to 0$.

Next, we introduce a function:

$$G(\delta, r, z) := \frac{1}{\pi}\int_{-R}^{R} du\, \frac{1}{\sqrt{(z - \delta + iu)^2 + r^2}} g(u). \tag{B3}$$

In terms of this function, the potential produced by $g(u)$ is just given by $G(d, r, z) - G(-d, r, z)$. Plugging Eq. (28) into Eq. (B3) with $\delta = \pm d$ and taking the NS5-brane limit (24), we obtain

$$G(\pm d, r, z) = G(\pm 3d, r, z) + \sum_{s=1}^{\Lambda} \frac{1}{\pi} \int_{-R_s}^{R_s} du \left(\frac{1}{\sqrt{(z \mp (2d + d_s) + iu)^2 + r^2}} - \frac{1}{\sqrt{(z \mp (2d - d_s) + iu)^2 + r^2}} \right) f_s(u), \tag{B4}$$

where we have used $C_{\Lambda+1} - C^{(0)} \to 0$ and the following relation that holds as $R \to \infty$:

$$\int_{-1}^{1} du \frac{1}{\sqrt{(z + iu)^2 + r^2}} K_s(\delta) f_s(u) \to \int_{-R_s}^{R_s} du' \frac{1}{\sqrt{(z + \mathrm{sgn}(z)\delta + iu')^2 + r^2}} f_s(u'). \tag{B5}$$

Repeating this procedure ν times, we arrive at

$$G(\pm d, r, z) = G(\pm(2\nu + 1)d, r, z) \pm \sum_{n=1}^{\nu} \sum_{s=1}^{\Lambda} \frac{1}{\pi} \int_{-R_s}^{R_s} du \left(\frac{1}{\sqrt{(z - d_s \mp 2nd + iu)^2 + r^2}} - \frac{1}{\sqrt{(z + d_s \mp 2nd + iu)^2 + r^2}} \right) f_s(u). \tag{B6}$$

Note that one can show that $G(\delta, r, z)$ is finite even in the NS5-brane limit and that $G(\delta, r, z)$ is on the order of $1/\delta$ for sufficiently large δ. Thus, the first term on the right-hand side turns out to vanish as $\nu \to \infty$. From the $\nu \to \infty$ limit of this expression, we finally obtain relation (29).

C. Electrostatic action in the NS5-brane limit

In this appendix, we derive the action of the electrostatic system for LST by starting from the action for PWMM (32) and then taking the NS5-brane limit.

A tricky term in Eq. (32) involved in the derivation is the term of $C_{\Lambda+1}\sigma_{\Lambda+1}(r)$. This can be rewritten as

$$2C_{\Lambda+1} \int_0^\infty 2\pi r dr\, \sigma_{\Lambda+1}(r) = -\frac{1}{4\pi} C_{\Lambda+1} \int_{-\infty}^{\infty} dz \int_0^\infty 2\pi r dr \frac{z}{|z|} \triangle V_{\Lambda+1}(r, z).$$

Then, this $V_{\Lambda+1}$ can be divided into $V^{(0)}$ and $V_{s,n}$ by using Eq. (30); hence it becomes

$$2C_{\Lambda+1} \int_0^\infty 2\pi r dr\, \sigma_{\Lambda+1}(r) = 2C_{\Lambda+1} \int_0^\infty 2\pi r dr\, \sigma^{(0)}(r) \tag{C1}$$

because

$$\frac{z}{|z|} \triangle V_{s,n}(r, z) = -4\pi \sigma_s(r)(\delta(z - d_s - 2nd) - \delta(z + d_s - 2nd)) \tag{C2}$$

holds for $|n| \geq 1$ and its integration over z vanishes. However, in order to express the action for LST by $V_{s,n}(r, z)$ in a neat way, we rewrite Eq. (C1) as

$$2C_{\Lambda+1} \int_0^\infty 2\pi r dr\, \sigma_{\Lambda+1}(r) = 2C_{\Lambda+1} \int_0^\infty 2\pi r dr\, \sigma^{(0)}(r) - \frac{1}{4\pi} \int_{-\infty}^{\infty} dz \int_0^\infty 2\pi r dr \sum_{s=1}^{\Lambda} \sum_{\substack{n=-\infty \\ \neq 0}}^{\infty} C_s \frac{z}{|z|} \triangle V_{s,n}(r, z), \tag{C3}$$

by utilizing the fact that the integration of Eq. (C2) over z vanishes for arbitrary s when $|n| \geq 1$.

By substituting Eqs. (8), (31), and (C3) into Eq. (32) and gathering the terms relevant for $V_{s,n}(r, z)$ (or $f_s(u)$), we now obtain, up to surface terms,

$$\begin{aligned} S_{\rm es} = -\frac{1}{4}\int_{-\infty}^{\infty} dz \int_0^{\infty} rdr \Bigg[& -\sum_{s,n}\sum_{t,m} V_{s,n}(r,z) \triangle V_{t,m}(r,z) \\ & -2\sum_{s,n}\left(V_0\left(r^2 z - \frac{2}{3}z^3\right) + V^{(0)}(r,z) - C_s\frac{z}{|z|}\right) \triangle V_{s,n}(r,z)\Bigg] \\ & -2\sum_{s=1}^{\Lambda} C_s Q_s + S_{{\rm es},\Lambda+1}, \end{aligned} \tag{C4}$$

where $S_{{\rm es},\Lambda+1}$ is an irrelevant term:

$$\begin{aligned} S_{{\rm es},\Lambda+1} = -\frac{1}{4}\int_{-\infty}^{\infty} dz \int_0^{\infty} rdr \Bigg[& -\left(V_0\left(r^2 z - \frac{2}{3}z^3\right) + V^{(0)}(r,z)\right) \triangle V^{(0)}(r,z)\Bigg] \\ & + 2C_{\Lambda+1}\left(\int_0^{\infty} 2\pi r dr\, \sigma^{(0)}(r) - Q\right). \end{aligned}$$

By putting $C_s = \tilde{C}_s + C^{(0)}\frac{d_s}{d}$ and taking the NS5-brane limit (24), we obtain

$$\begin{aligned} S_{\rm es} = -\frac{1}{4}\int_{-\infty}^{\infty} dz \int_0^{\infty} rdr \Bigg[& -\sum_{s,n}\sum_{t,m} V_{s,n}(r,z) \triangle V_{t,m}(r,z) \\ & -2\sum_{s,n}\left(\frac{1}{g_0}\sin\frac{\pi z}{d} I_0\left(\frac{\pi r}{d}\right) - \tilde{C}_s\frac{z}{|z|}\right) \triangle V_{s,n}(r,z)\Bigg] - 2\sum_{s=1}^{\Lambda}\tilde{C}_s Q_s, \end{aligned} \tag{C5}$$

up to irrelevant constants. One can see that this gives the action of the electrostatic potential for LST. In terms of the charge densities $f_s(u)$, it is rewritten as

$$\begin{aligned} S_{\rm es} = -\frac{2}{\pi}\Bigg[& \sum_{s=1}^{\Lambda}\sum_{n=-\infty}^{\infty}\frac{1}{2}\int du\, f_s(u)^2 \\ & -\sum_{s,n}\sum_{t,n'}\frac{1}{2\pi}\int du du'\Bigg[\frac{|d_s + d_t + 2n'd|}{(d_s + d_t + 2n'd)^2 + (u-u')^2} \\ & -\frac{|d_s - d_t + 2n'd|}{(d_s - d_t + 2n'd)^2 + (u-u')^2}\Bigg] f_s(u) f_t(u') \\ & +\frac{1}{g_0}\sum_{s,n}\sin\frac{\pi d_s}{d}\int du\cosh\frac{\pi u}{d} f_s(u) - \sum_{s=1}^{\Lambda}\tilde{C}_s\left(\int du\, f_s(u) - \pi Q_s\right)\Bigg]. \end{aligned} \tag{C6}$$

It is easily seen that the equation of motion for $f_s(u)$ coincides with the integral equation of $\tilde{f}_s(u)$ in Eq. (15). Thus, in the limit (24), the action of the electrostatic system for PWMM indeed reduces to the action for LST.

D. Details of numerical analysis

In this appendix, we show our choice of the parameters for the numerical computation in Sect. 5.2.

Table D1. $N_2^{(2)}$ and λ (= 200, 300, 400, and 500), which we choose in our simulations. The cell whose row and column are λ and $N_2^{(2)}$, respectively, indicates the corresponding value of $\tilde{g}_s$ computed through Eq. (61).

$\lambda \backslash N_2$	70	80	90	100	110	120	130	140	150	200	300
200	10.75	9.40	8.36	7.52	6.84	6.27	5.79	5.37	5.02	3.76	2.51
300	19.71	17.25	15.33	13.80	12.54	11.50	10.61	9.86	9.20	6.90	4.60
400	31.01	27.13	24.12	21.71	19.73	18.09	16.70	15.50	14.47	10.85	7.24
500	44.69	39.10	34.76	31.28	28.44	26.07	24.06	22.34	20.85	15.64	10.43

Table D2. $N_2^{(2)}$ and λ (= 600, 700, 800, and 900), which we choose in our simulations. Again, each cell in the body of the table indicates the corresponding value of $\tilde{g}_s$ computed through Eq. (61).

$\lambda \backslash N_2$	70	90	110	130	150	200	300	400	500
600	60.81	47.30	38.70	32.75	28.38	21.29	14.19	–	–
700	79.47	61.81	50.57	42.79	37.09	27.81	18.54	–	–
800	100.75	78.36	64.11	54.25	47.01	35.26	23.51	17.63	–
900	–	97.01	79.37	67.16	58.21	43.66	29.10	21.83	17.46

D.1. Parameter region for the NS5-brane limit

The expectation values are computed with

$$N_2^{(2)} = 20, 40, 60, 80, 100 \tag{D1}$$

at each fixed value of $\tilde{g}_s = 100, 200, 300, 400, 500$. We choose the other fixed parameters as $D_1 = N_5^{(1)} = 1$, $D_2 = D = 2$, and $N_2^{(1)} = 4$. These are chosen so that $\lambda \gg D^4$ in Eq. (42), which is actually required by the NS5-brane limit (61) as λ scales as $(D \ln N_2^{(2)})^4$ and hence $\lambda \gg D^4$.

Note, however, that D_1 and $D_2 - D_1$ are not large but 1 in this case. Thus we expect that the system reproduces the theory on two NS5-branes with a D2-brane flux, which should contain substantial string and quantum corrections. This is not a problem because the purpose of the simulation is to confirm the double scaling limit.

D.2. Parameter region for the large-N limit

We compute the expectation values by setting the parameters $N_2^{(2)}$ and $\lambda = g^2 N_2^{(2)}$ to the values listed in Tables D1 and D2. These tables show the corresponding $\tilde{g}_s$ obtained by Eq. (61).

We choose the other fixed parameters as $D_1 = N_5^{(1)} = 3$, $D_2 = D = 6$, and $N_2^{(1)} = 4$. Again, λ needs to satisfy $\lambda \gg D^4$. Since it is a stringent condition for numerical simulations due to costly computation of such large-size matrices, we choose the region of λ to be $\lambda > D^4/8 = 162$.

D.3. Coefficients $d_0(\lambda)$ and $d_1(\lambda)$

Here, we show the obtained data of $d_0(\lambda)$ and $d_1(\lambda)$ for $\langle \mathrm{Tr} M_1^2 \rangle_M$ in Table D3. We perform large-N_2 extrapolation, namely, fitting by a quadratic function $a + b/N_2 + c/(N_2)^2$ where a, b, c are free parameters and $N_2 = N_2^{(2)}$. As a result of the fitting, we identify a, b with $d_0(\lambda)$ and $d_1(\lambda)$, respectively.

Table D3. The coefficients of $\langle \mathrm{Tr} M_1^2 \rangle_M$.

λ	$d_0(\lambda)$	$d_1(\lambda)$
200	0.17(1)	0.236(5)
300	0.28(3)	0.193(5)
400	0.36(5)	0.170(5)
500	0.64(6)	0.139(5)
600	0.73(8)	0.130(5)
700	0.82(11)	0.139(5)
800	0.84(8)	0.115(3)
900	0.93(8)	0.110(3)

Table D4. The coefficients of $\langle \mathrm{Tr} M_1^2 \rangle_M$.

	$\tilde{g}_s \leq 50$		$\tilde{g}_s \leq 60$	
λ	$d_0(\lambda)$	$d_1(\lambda)$	$d_0(\lambda)$	$d_1(\lambda)$
600	0.63(1)	0.139(8)	0.63(1)	0.139(8)
700	0.5(3)	0.14(2)	0.4(2)	0.15(1)
800	0.7(2)	0.13(2)	0.7(2)	0.13(1)
900	1.1(3)	0.10(2)	1.1(3)	0.10(2)

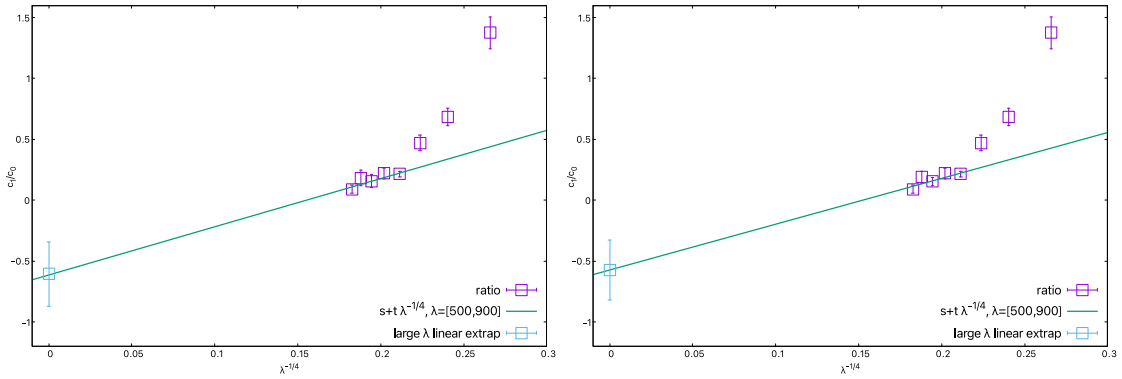

(a) $\tilde{g}_s \leq 50$ (b) $\tilde{g}_s \leq 60$

Fig. D1. A plot of the ratio c_1/c_0 of $\langle \mathrm{Tr} M_1^2 \rangle_M$. At each data point of λ, we restrict $\tilde{g}_s \leq 50$ in (a) and $\tilde{g}_s \leq 60$ in (b) for the extrapolation. The horizontal axis is $\lambda^{-1/4}$. The green lines are the fitted lines by $s + t\lambda^{-1/4}$, where s and t are fitting parameters. The blue square at $\lambda^{-1/4} = 0$ shows the extrapolated value of c_1/c_0 by the 't Hooft limit.

D.4. Comparison with $\tilde{g}_s$

We perform the large-λ extrapolation varying the range of $\tilde{g}_s$ and compare the dependence of the range. See Table D4 for the best fit parameters fitted in the ranges $\tilde{g}_s \leq 50$ and $\tilde{g}_s \leq 60$, and see Fig. D1 for the plot of the data.

Below $\lambda = 500$, the restriction for $\tilde{g}_s$ provides no condition. For $\lambda = 600$, the restriction gives the same condition and hence the same coefficients for the fit. The error tends to be bigger than the one without restriction due to the reduction of the data points for the fit.

References

1 J. M. Maldacena, Adv. Theor. Math. Phys. **2**, 231 (1998).
2 S. S. Gubser, I. R. Klebanov, and A. M. Polyakov, Phys. Lett. B **428**, 105 (1998).
3 E. Witten, Adv. Theor. Math. Phys. **2**, 253 (1998).
4 O. Aharony, Classical Quantum Gravity **17**, 929 (2000) [arXiv:hep-th/9911147] [Search inSPIRE].
5 D. Kutasov, ICTP Lect. Notes Ser. **7**, 165 (2002).
6 D. E. Berenstein, J. M. Maldacena, and H. S. Nastase, J. High Energy Phys. **0204**, 013 (2002).
7 H. Lin and J. M. Maldacena, Phys. Rev. D **74**, 084014 (2006) [arXiv:hep-th/0509235] [Search INSPIRE].
8 H. Ling, A. R. Mohazab, H.-H. Shieh, G. van Anders, and M. Van Raamsdonk, J. High Energy Phys. **0610**, 018 (2006) [arXiv:hep-th/0606014] [Search inSPIRE].
9 H. Lin, O. Lunin, and J. M. Maldacena, J. High Energy Phys. **0410**, 025 (2004) [arXiv:hep-th/0409174] [Search INSPIRE].
10 G. Ishiki, S. Shimasaki, Y. Takayama, and A. Tsuchiya, J. High Energy Phys. **0611**, 089 (2006).
11 G. Ishiki, Y. Takayama, and A. Tsuchiya, J. High Energy Phys. **0610**, 007 (2006).
12 J. Maldacena, M. M. Sheikh-Jabbari, and M. Van Raamsdonk, J. High Energy Phys. **0301**, 038 (2003) [arXiv:hep-th/0211139] [Search inSPIRE].
13 H. Ling, H.-H. Shieh, and G. van Anders, J. High Energy Phys. **0702**, 031 (2007).
14 Y. Asano, G. Ishiki, T. Okada, and S. Shimasaki, J. High Energy Phys. **1405**, 075 (2014).
15 Y. Asano, G. Ishiki, and S. Shimasaki, J. High Energy Phys. **1409**, 137 (2014).
16 Y. Asano, G. Ishiki, S. Shimasaki, and S. Terashima, Phys. Rev. D **96**, 126003 (2017).
17 Y. Asano, G. Ishiki, S. Shimasaki, and S. Terashima, J. High Energy Phys. **1802**, 076 (2018).
18 D. Roychowdhury, arXiv:2110.05395 [hep-th] [Search inSPIRE].
19 G. van Anders, J. High Energy Phys. **0703**, 028 (2007) [arXiv:hep-th/0701277] [Search INSPIRE].
20 V. Pestun, Commun. Math. Phys. **313**, 71 (2012).
21 Y. Asano, G. Ishiki, T. Okada, and S. Shimasaki, J. High Energy Phys. **1302**, 148 (2013).